

LETTER • OPEN ACCESS

Accelerated decline of summer Arctic sea ice during 1850–2017 and the amplified Arctic warming during the recent decades

To cite this article: Qiongqiong Cai *et al* 2021 *Environ. Res. Lett.* **16** 034015

View the [article online](#) for updates and enhancements.

You may also like


- [Ultrafast Arctic amplification and its governing mechanisms](#)
Tyler P Janoski, Michael Previdi, Gabriel Chiodo et al.
- [A recent weakening of winter temperature association between Arctic and Asia](#)
Bingyi Wu, Zhenkun Li, Jennifer A Francis et al.
- [Circumpolar Arctic vegetation: a hierarchic review and roadmap toward an internationally consistent approach to survey, archive and classify tundra plot data](#)
D A Walker, F J A Daniëls, I Alsos et al.

ENVIRONMENTAL RESEARCH
LETTERS

LETTER

Accelerated decline of summer Arctic sea ice during 1850–2017
and the amplified Arctic warming during the recent decades

OPEN ACCESS

RECEIVED
19 June 2020REVISED
4 January 2021ACCEPTED FOR PUBLICATION
13 January 2021PUBLISHED
19 February 2021Qiongqiong Cai^{1,2}, Jia Wang³, Dmitry Beletsky², James Overland⁴ , Moto Ikeda⁵ and Liying Wan¹¹ National Marine Environmental Forecasting Center (NMEFC), Ministry of Natural Resources, Beijing, People's Republic of China² Cooperative Institute for Great Lakes Research (CIGLR), School for Environment and Sustainability, University of Michigan, Ann Arbor, MI, United States of America³ Great Lakes Environmental Research Laboratory, NOAA, Ann Arbor, MI, United States of America⁴ Pacific Marine Environmental Laboratory, NOAA, Seattle, WA, United States of America⁵ Hokkaido University, Sapporo, JapanE-mail: jia.wang@noaa.gov**Keywords:** trends of summer Arctic sea ice variations, global warming, internal variability of the climate system, Arctic temperature amplificationOriginal content from
this work may be used
under the terms of the
[Creative Commons
Attribution 4.0 licence](https://creativecommons.org/licenses/by/4.0/).Any further distribution
of this work must
maintain attribution to
the author(s) and the title
of the work, journal
citation and DOI.**Abstract**

The 168 year trends of summer (July–September) sea ice area (SIA) variations in six Arctic regions during 1850–2017 are analyzed. SIA has been significantly decreasing in most Arctic regions since 1850. The rate of retreat for the period of 1948–2017 accelerated multi-fold. For the nearly four decades since 1979, most Arctic regions are experiencing the highest reduction rate. Besides the increasing surface air temperature, the key drivers to the accelerated summer Arctic sea ice decline are found to be the combined global warming and the regional Arctic warming exerted simultaneously by the Arctic Oscillation, North Atlantic Oscillation, Atlantic Multidecadal Oscillation and Pacific Decadal Oscillation during the last several decades. The dynamical and thermodynamical warming, driven by the internal variability of the teleconnection patterns, occurred in the last several decades, in particular on the multidecadal timescales. This leads to Arctic amplification that accelerates the positive ice/ocean albedo feedback loop, resulting in accelerating summer sea ice decline.

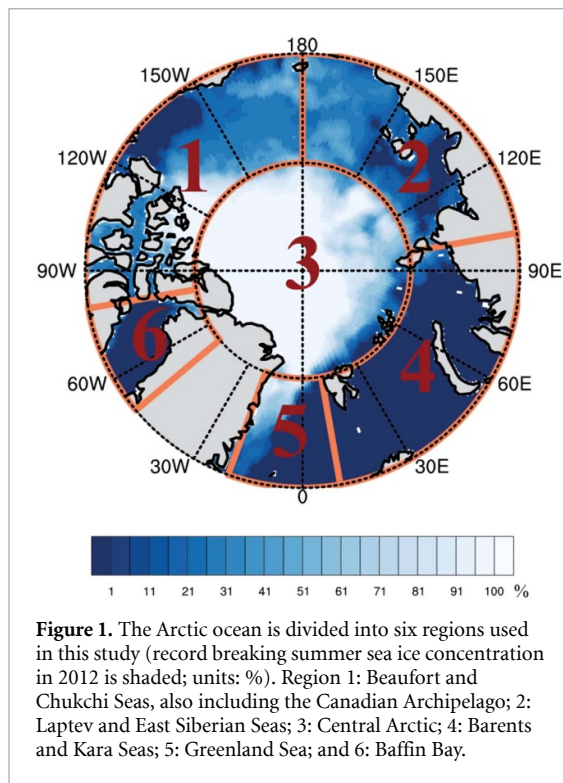
1. Introduction

Arctic sea ice plays an important role in the climate system. It is sensitive to climate change and strongly affects the atmospheric energy budget, ocean circulation, and air–sea interactions (Walsh 1983, Mysak *et al* 1990, Deser *et al* 2000). The persistent decline in annual sea ice cover, which can lead to unprecedented changes in the global climate, has been well documented since the 1980s (Stroeve *et al* 2012, Schweiger *et al* 2019).

Various studies have shown that the warming air temperature (Stroeve *et al* 2007, Polyakov *et al* 2012) resulting from the increased downward infrared radiation (Ikeda *et al* 2003, Kapsch *et al* 2016) and positive ice/ocean albedo feedback (Wang *et al* 2005, Screen and Simmonds 2010, Lei *et al* 2016), anomalous ocean currents (Kinnard *et al* 2011), anomalous wind forcing (Ogi *et al* 2010), northward transport of atmospheric moisture and

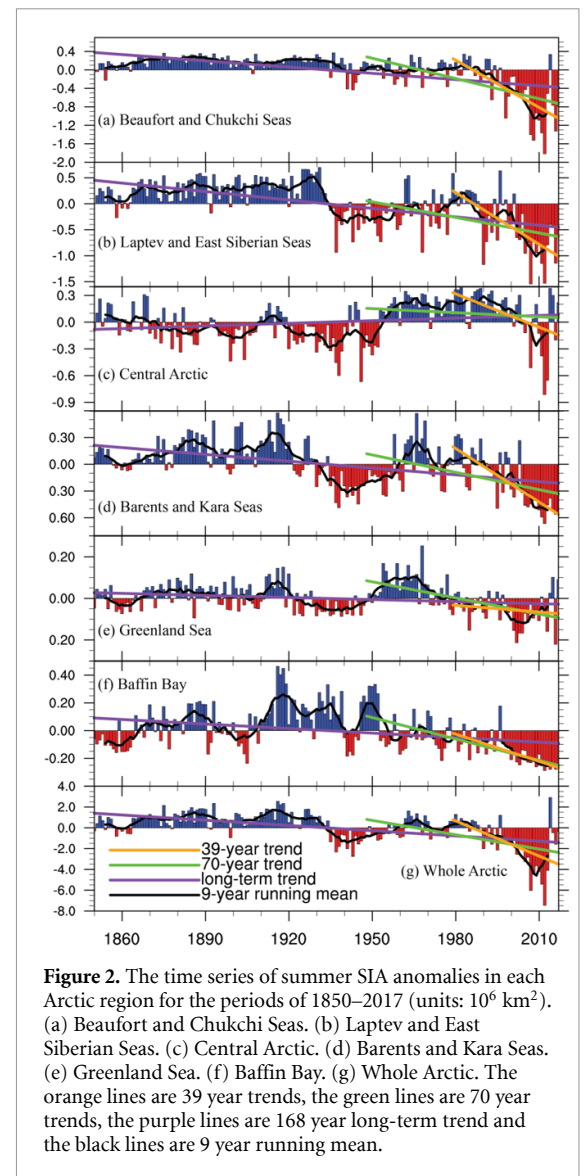
sensible heat (Park *et al* 2015, Hegyi and Taylor 2018), and some dominant patterns of atmospheric circulation variability such as Arctic dipole anomaly (DA) (Wang and Ikeda 2000, Overland and Wang 2005, 2015, Wang *et al* 2009) are recognized as the possible key drivers of rapid Arctic sea ice loss.

This study examines the longest (168 year) summer sea ice area (SIA) time series regarding trend and variability. Compared with other studies (Alekseev *et al* 2016, Connolly *et al* 2017), the detailed geographical features in six Arctic regions are more emphasized (figure 1). Based on the evaluation of trends for different periods (1850–2017, 1948–2017 and 1979–2017), the impacts of global warming and dominant internal climate variability on the accelerated sea ice decline in the recent decades are further investigated, which was due to the accelerated positive ice/ocean albedo feedback at work (Wang *et al* 2005, 2014).



2. Data and methods

The SIA data is the sum of the grid cell areas multiplied by the ice concentration (Peng *et al* 2013, Meier *et al* 2017, Walsh *et al* 2017) from the National Snow and Ice Data Center (NSIDC). The dataset consists of two types of measurements: traditional ship-based and airborne before 1979 and satellite-based since 1979. The data from 1900–1978 were merged to a gridded dataset (Chapman and Walsh 1993), which has been used by previous studies (Wang and Ikeda 2000, 2001, and many others). Using the same approach, Walsh *et al* (2017) further synthesized Arctic sea ice data from a variety of historical sources into the database, extending it back to 1850 with monthly time-resolution. The synthesis procedure includes interpolation to a uniform grid and an analog-based estimation of ice concentrations in areas of no data. Large uncertainty may exist in the data prior to 1979 and, in terms of mean, its systematic error should differ from that of the satellite era. However, in this study we investigate the variability rather than the mean, similar to Wang and Ikeda (2001) and Wang *et al* (2005), who used the dataset for analysis of sea ice variability and trend during the period 1900–1995. Brennan *et al* (2020) pointed out that the lower interannual variability during the instrumental era is mainly due to a lack of high quality sea ice observations in the early 20th-century warming (ETCW; 1918–1948) in this dataset. Therefore, we evaluated and compared the trends of 1850–2017, 1948–2017 and 1979–2017, respectively.



We mainly focus on the analysis in summer because that is the time period in which SIA reaches the minimum value (July–September) and high standard deviations usually occur (Wang and Ikeda 2001), indicating that summer ice cover can capture major interannual and decadal variability. The time series of summer SIA anomalies are calculated by removing the summer climatology (figure 2). The summer Arctic surface air temperature (SAT) time series (1850–2017; Morice *et al* 2012) is the standardized July–September averaged SAT anomalies over 70°–90° N by using HadCRUT4 from the Climatic Research Unit (University of East Anglia) and Hadley Centre (UK Met Office). For composite analysis (figure 4), the SAT is from the NOAA-CIRES Twentieth Century Reanalysis version 3 (1836–2015; 20CRv3; Slivinski *et al* 2019).

By applying empirical orthogonal functions (EOFs) to the normalized Arctic (70°–90° N) sea level pressure (SLP; 1948–2017) from the National

Table 1. The linear decadal rates of summer SIA (unit: $10^6 \text{ km}^2 \text{ decade}^{-1}$; at the 99% significance level) and trend percentages (shown in parentheses; unit: per decade; relative to the 1979–2017 average) in each region over the periods of 1850–2017, 1948–2017, and 1979–2017.

Unit: $10^6 \text{ km}^2 \text{ decade}^{-1}$	168 year trend (1850–2017)	70 year trend (1948–2017)	39 year trend (1979–2017)
1. Beaufort and Chukchi Seas (B&C)	−0.045 (− 1.51%)	−0.15 (− 5.02%)	−0.34 (− 11.37%)
2. Laptev and East Siberian Seas (L&E.S)	−0.054 (− 2.83%)	−0.10 (− 5.24%)	−0.33 (− 17.28%)
3. Central Arctic (C.Ar)	0.010 (0.14%)	−0.015 (− 0.21%)	−0.12 (− 1.70%)
4. Barents and Kara Seas (B&K)	−0.025 (− 4.72%)	−0.065 (− 12.26%)	−0.20 (− 37.74%)
5. Greenland Sea (Gre.)	−0.0033 (− 1.43%)	−0.026 (− 11.30%)	−0.011 (− 4.78%)
6. Baffin Bay (Baf.)	−0.011 (− 5.50%)	−0.052 (− 26.00%)	−0.065 (− 32.50%)
7. Whole Arctic	−0.17 (− 0.96%)	−0.46 (− 2.60%)	−1.10 (− 6.22%)

All the rates are statistically significant at the 99% level and the trend percentages in parentheses are shown in bold for highlight.

Table 2. The correlation coefficient between summer SIA (left: SIA with long-term trend; right: SIA without long-term trend) and summer Arctic air temperature, summer AO, summer DA, winter NAO, AMO and summer PDO in each region (The 95% significance levels in bold are determined by Monte Carlo simulation.).

	Arctic SAT (1850–2017)		AO (1948–2017)		DA (1948–2017)		NAO (1865–2017)		AMO (1856–2017)		PDO (1854–2017)	
B&C	−0.57	−0.30	0.05	0.10	−0.27	−0.28	−0.14	−0.12	−0.29	−0.37	0.15	0.15
L&E.S	−0.60	−0.35	−0.01	0.05	−0.36	−0.37	−0.13	−0.10	−0.26	−0.32	0.15	0.16
C.Ar	−0.06	−0.17	0.03	0.01	−0.10	−0.11	0.09	0.07	−0.20	−0.20	0.17	0.19
B&K	−0.61	−0.39	−0.12	−0.08	−0.16	−0.16	−0.07	−0.04	−0.34	−0.39	0.09	0.08
Gre.	−0.38	−0.27	−0.26	−0.25	0.12	0.13	−0.05	−0.03	−0.14	−0.15	−0.01	−0.02
Baf.	−0.39	−0.22	−0.27	−0.25	−0.11	−0.11	−0.15	−0.14	−0.14	−0.15	−0.01	−0.03
Arctic	−0.62	−0.39	−0.01	0.04	−0.27	−0.28	−0.07	−0.03	−0.31	−0.37	0.18	0.19

Centers for Environmental Prediction National Center for Atmospheric Research (NCEP/NCAR) reanalysis I dataset (Kalnay *et al* 1996), the leading mode is Arctic Oscillation (AO) and the second mode is named Arctic DA pattern (Overland and Wang 2005, Wu *et al* 2006, Wang *et al* 2009). The station-based North Atlantic Oscillation (NAO) index (1865–2017; Hurrell 1995) is the difference of normalized SLP between Lisbon, Portugal and Stykkisholmur/Reykjavik, Iceland and obtained from the NCAR's Climate Analysis section. The Atlantic Multidecadal Oscillation (AMO) index (1856–2017; Enfield *et al* 2001) is computed as the area weighted average sea surface temperature (SST) over the North Atlantic and further detrended from the NOAA Earth System Research Laboratory. The Pacific Decadal Oscillation (PDO) index (1854–2017; Mantua *et al* 1997) as the leading (EOF) mode of North Pacific (20° – 70° N) SST monthly averaged anomalies are from NOAA's National Centers for Environmental Information. Since summer AO, summer DA, winter (January–March) NAO, and summer PDO show better correlations with the summer SIA variation compared to other seasons, only these seasonal indices are shown in this study. Though there are quantitative differences among different seasons, the main results are in good agreement regardless of seasons.

Trends for the yearly SIA are calculated using linear least squares regression and the Student's *t*-test is used for the significance (table 1). The Monte Carlo

simulation (Wang and Ikeda 2000) is used for the correlation evaluation (table 2).

3. Regional summer Arctic sea ice variations

The time series of summer SIA anomalies show the pronounced interannual and decadal variations (figure 2). However, there is less variability prior to the satellite era (except for Baffin Bay; Alekseev *et al* 2016, Connolly *et al* 2017), a significant part of which is due to a lack of high quality sea ice observations in the ETCW (Brennan *et al* 2020). The Beaufort, Chukchi, Laptev, East Siberian, Barents, Kara and Greenland Seas and the whole Arctic experienced a sharp shift from the positive phase to the negative phase between the 1930s and 1940s (figures 2(a), (b), (d), (e) and (g)), which is the same as the results of the reconstructed dataset from Alekseev *et al* (2016) and Connolly *et al* (2017). The Central Arctic exhibited a transition from negative to positive phase in 1952–1953 (figure 2(c)). The generally increasing SIA from mid 1940s until late 1970s only occurs in the Greenland Sea (figure 2(e); Pirón and Pasalodos 2016, Alekseev *et al* 2016, Connolly *et al* 2017). Except for the Central Arctic, the summer SIA has been generally decreasing since the late 1970s.

The summer SIA anomalies in most Arctic regions (except for the Central Arctic) have been, statistically, significantly decreasing

since 1850 (figure 2 and table 1). The largest decreasing linear trend of -5.50% decade $^{-1}$ (-0.011×10^6 km 2 decade $^{-1}$) occurs in Baffin Bay. The Greenland Sea shows the smallest negative trend of -1.43% decade $^{-1}$ (-0.0033×10^6 km 2 decade $^{-1}$). A reversed trend toward increasing SIA in the Central Arctic over the 168 years is apparent. For the whole Arctic, the overall rate of change is -0.96% decade $^{-1}$ (-0.17×10^6 km 2 decade $^{-1}$) during 1850–2017.

The declining trend has accelerated since 1948 and more than doubled compared to the long-term trend (table 1) over the Beaufort and Chukchi Seas (-5.02% decade $^{-1}$ (-0.15×10^6 km 2 decade $^{-1}$)), (Laptev and East Siberian Seas (-5.24% decade $^{-1}$ (-0.10×10^6 km 2 decade $^{-1}$)), Barents and Kara Seas (-12.26% decade $^{-1}$ (-0.065×10^6 km 2 decade $^{-1}$)) and Baffin Bay (-26% decade $^{-1}$ (-0.052×10^6 km 2 decade $^{-1}$)). The Greenland Sea trend has increased nearly sevenfold and exhibited the most rapid decline (-11.30% decade $^{-1}$). In the Central Arctic, the 70 year (1948–2017) trend has translated into a statistically significant negative trend of -0.21% decade $^{-1}$ (-0.015×10^6 km 2 decade $^{-1}$). The decline in the whole Arctic has increased 1.7 times at the rate of -2.60% decade $^{-1}$ (-0.46×10^6 km 2 decade $^{-1}$) since 1948.

Most Arctic regions (except for the Greenland Sea) have experienced the highest reduction of SIA over the last nearly 4 decades, since 1979. During the 39 year period, the trends have more than doubled over the Beaufort and Chukchi Seas (-11.37% decade $^{-1}$ (-0.34×10^6 km 2 decade $^{-1}$)), Laptev and East Siberian Seas (-17.28% decade $^{-1}$ (-0.33×10^6 km 2 decade $^{-1}$)) and Barents and Kara Seas (-37.74% decade $^{-1}$ (-0.20×10^6 km 2 decade $^{-1}$)). The fastest decrease in SIA over the Central Arctic (-1.70% decade $^{-1}$) is seven times faster than the trend for the 70 year (1948–2017) period. For the whole Arctic, the decline has reached -6.22% decade $^{-1}$ (-1.10×10^6 km 2 decade $^{-1}$)—more than double the 70 year trend.

The accelerated decline in SIA in recent decades was due to both dynamical forcing (such as positive Arctic DA whose associated anomalous meridional wind effectively advects sea ice out of the Arctic via enhancing the Transpolar Drift Stream (see figure 2 of Wang *et al* 2009)) and thermodynamical effect, such as temperature amplification (see figure 4.18 of Wang 2014). In particular, the Arctic amplification has been attributed to a number of mechanisms, namely, sea ice albedo feedback (Wang *et al* 2005, Screen and Simmonds 2010, 2014), temperature feedbacks (Pithan and Mauritsen 2014), external global warming (Min *et al* 2008), large-scale atmospheric circulation variability of the internal climate system (Ding *et al* 2017, Mewes and Jacobi 2019), changes to the radiation balance (Graversen and Burtu 2016) and enhanced surface fluxes (Boisvert *et al* 2015).

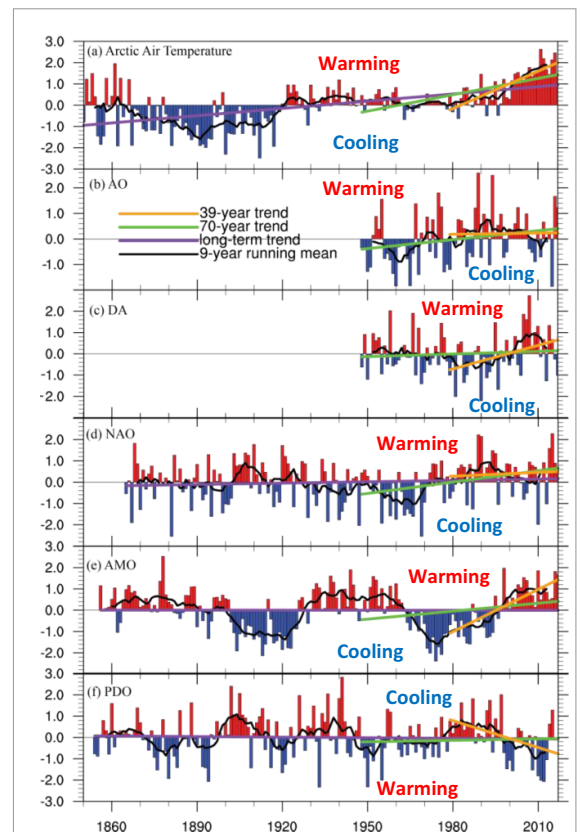


Figure 3. The standardized time series of climate indices. (a) Summer Arctic air temperature. (b) Summer AO. (c) Summer DA. (d) Winter NAO. (e) AMO. (f) Summer PDO. The orange lines are 39 year trends, the green lines are 70 year trends, the purple lines are long-term trends and the black lines are 9 year running means. The ‘warming’ and ‘cooling’ presents the positive and negative SAT anomalies over the most Arctic seas for different phase based on figure 4.

4. Association between summer Arctic sea ice and dominant climate variability

The Arctic SAT record (Morice *et al* 2012) in summer shows a sustained cooling phase over the first 70 years as the result of Kinnard *et al* (2011), followed by the ETCW (1920s–1940s). Then, the Arctic went through a slight cooling (1940s–1970s), followed by another period of warming (1970s–present; figure 3(a)). With the accelerated warming trend of 0.59 K decade $^{-1}$ in recent decades, the air temperature has increased by 2.24 K since 1979. Except for the Central Arctic, the correlation with SIA is statistically significant and the coefficient with the detrended SIA is reduced more than 30% (table 2), indicating that change in SAT is a critical mechanism, actively contributing to the accelerated decline of SIA in the Arctic (Vinnikov *et al* 1999).

AO and Arctic DA are the first two leading modes of SLP anomalies in the Arctic (Overland and Wang 2005, Wu *et al* 2006, Wang *et al* 2009). In summer, both indices display large interannual and decadal fluctuations with weak increasing trend (figures 3(b)

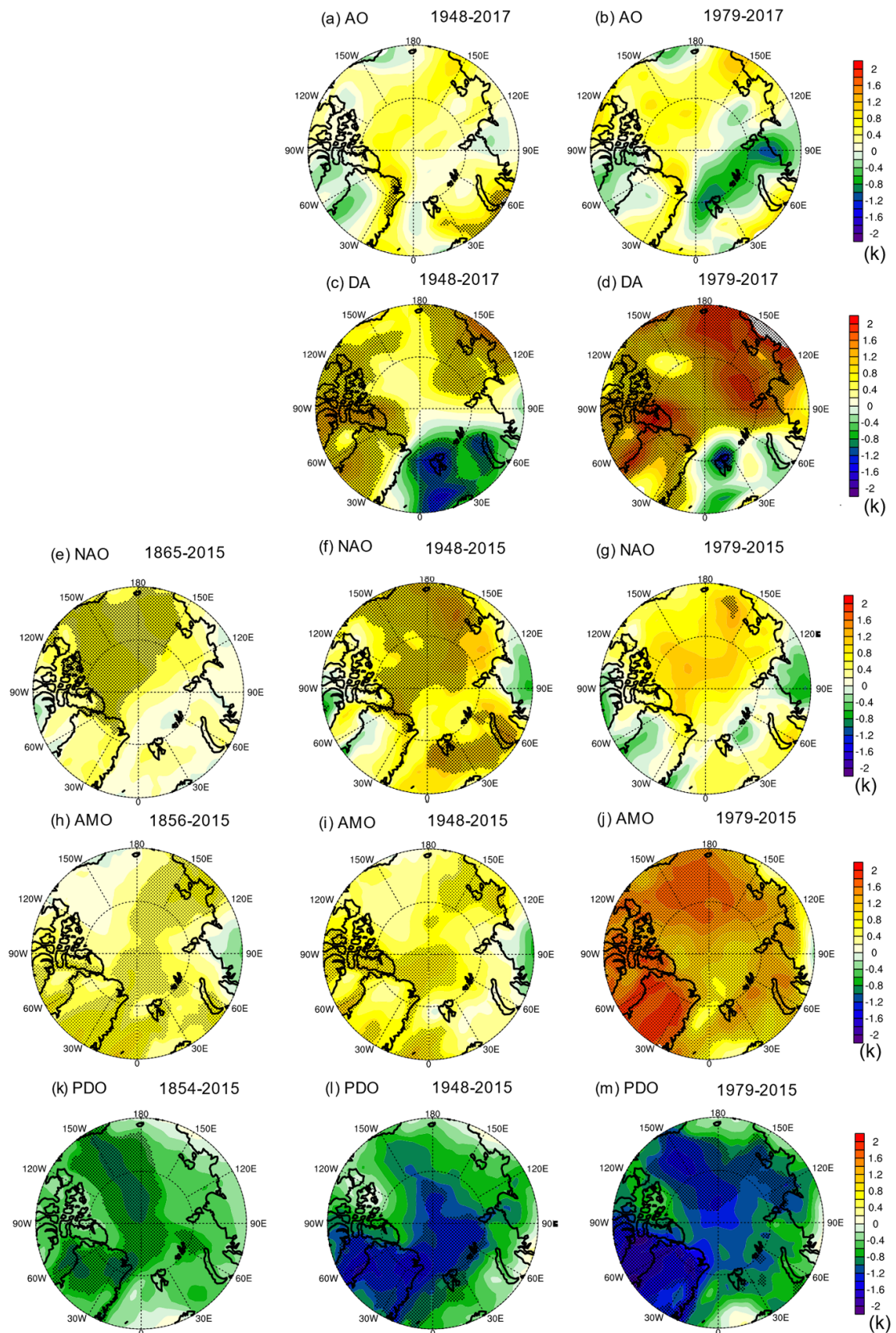


Figure 4. The differences of composited SAT anomalies (unit: K) between positive and negative events (one STD) during (left) 1800s–2015, (middle) 1948–2015 and (right) 1979–2015 for (a) AO (a) and (b), DA (c) and (d), NAO (e)–(g), AMO (h)–(j), and PDO (k)–(m). The regions above 95% confidence level are stippled. Based on figure 3, all five teleconnections had simultaneous warming for most Arctic regions in the recent decades, contributing to the Arctic temperature amplification, in addition to the overall global/Arctic warming impact.

and (c)). AO (DA) shows higher correlation with SIA in the Atlantic (Pacific) Ocean (table 2). The correlation between summer AO and SIA becomes smaller in most regions after removing the long-term trend of summer SIA. However, the correlation between summer DA and the detrended summer SIA slightly increases in the Arctic regions. It indicates that DA has a much stronger relationship with the natural variability of SIA (Wang *et al* 2009) than the AO (Rigor 2002). DA (AO) has had a positive (warming in most Arctic regions) trend in the last two (four) decades (figures 3(b) and (c)), however the time span is relatively short compared with others.

NAO (Hurrell 1995) is one of the most prominent teleconnection patterns in all seasons (Livezey and Mo 1987, Gong and Luo 2017). The winter index exhibits considerable interannual variability and the increasing trend during 1948–2017 is more significant than that during 1865–2017 and 1979–2017 (figure 3(d)). It is found that the winter NAO shows relatively higher correlation with the summer SIA variations, and greatly weakens when removing the trend of SIA (table 2), which means NAO is well-related to the recent greater retreating rate of SIA in the Arctic. NAO underwent a positive (warming) trend in the last four decades (figure 3(d)).

The SST-based AMO index (Enfield *et al* 2001) provides a simple and concise way to describe Atlantic multidecadal variability. This long-term detrended record nearly covers two cycles, with increasing trend in the recent decades (figure 3(e)). After removing the linear trend from the summer SIA time series, the correlations become larger (table 2), which means AMO is better correlated to the natural variability of summer SIA. AMO has experienced the largest warming in the last two decades (figure 3(e)).

The PDO (Mantua *et al* 1997), as a long-lived pattern of Pacific SST variability, has a significant influence on the climate of the Arctic (Screen and Francis 2016). The summer index shows strong interannual and decadal variations with no significant long-term (1854–2017) trend (figure 3(f)). However, with recent, more negative values in the 21st century, there has been a downward trend since 1979. The correlation between the PDO and the detrended summer SIA has become larger in most regions (table 2), suggesting that PDO correlates with the natural variability of SIA. However, the small correlation coefficients suggest that summer PDO plays a relatively small role on the accelerated decreasing rate of SIA, compared to the summer AMO. PDO showed a negative (warming) phase in the last two decades (figure 3(f)).

To further highlight how the five teleconnection patterns impact Arctic SAT anomalies, composite analyses with Student's *t*-tests are used to confirm the significantly impacted regions. Figure 4 shows that during the positive phase of AO, DA, NAO, and AMO, and negative of PDO, the Arctic SAT experiences warming anomaly in most Arctic regions, and

vice versa. DA, AMO and PDO have more significant (over 95%) impacts over the pan-Arctic, with AMO being most significant. Positive AO causes a relatively weak warming among all Arctic seas (figures 4(a) and (b)). It is noted that +DA, a local mode, causes warming in the Pacific and Central Arctic, and cooling in the Atlantic Arctic, and vice versa during –DA (figures 4(c) and (d)). Similar to the AO, during the positive NAO phase, the composite SAT shows warming anomalies among all Arctic seas (figures 4(e)–(g)). The positive AMO exhibits the overall Arctic warming (figures 4(h)–(j)). Negative (positive) PDO causes significant warming (cooling) along Baffin Bay. The amplitude became larger in the recent decades (1979–2015; figures 4(b), (d), (g), (j) and (m)), indicating the stronger positive phase of AO, DA, NAO, AMO and negative phase of PDO (see figure 3) simultaneously contributed to the Arctic amplification. However, we are cognizant that our results are based on fully statistical methods and that the understanding of the causal relationship requires dynamical modeling with coupled atmosphere–ocean–sea ice models, which remains an important topic for future research.

5. Conclusion

Using the longest (1850–2017) gridded sea ice data available, our study presents the long-term (168 year) trend in six Arctic regions and further compares the trends for the periods of 1948–2017 and 1979–2017, indicating that the declining trend has accelerated since 1948 and most Arctic regions (except for the Greenland Sea) have experienced the highest reduction of SIA over the last nearly 4 decades. This analysis suggests that the accelerated decline of SIA in recent decades was not uniquely driven by a single factor, but by a combination of global warming and internal variability of the climate system, particularly on the multidecadal timescales, which contributed to Arctic temperature amplification and anomalous atmospheric and oceanic circulation patterns over the pan-Arctic. The Arctic temperature amplification (Screen and Francis 2016) and oceanic and atmospheric dynamical and thermodynamical processes directly and indirectly accelerate the temperature feedbacks and the positive ice/ocean albedo feedback loop (Mysak *et al* 1990, Wang *et al* 2005, 2014), leading to the accelerating decline of summer Arctic sea ice.

Data availability statement

All data used in analysis available in public repositories. The sea ice concentration data is downloaded from <http://nsidc.org/data/g10010>, <http://nsidc.org/data/G02202> and <http://nsidc.org/data/G10016>. The HadCRUT4 near surface temperature data set is from www.metoffice.gov.uk/hadobs/hadcrut4/data/current/download.html, 20CRv3 is

from https://psl.noaa.gov/thredds/catalog/Datasets/20thC_ReanV3/Monthlies/catalog.html, NCEP1 SLP is from www.esrl.noaa.gov/psd/data/gridded/data.ncep.reanalysis.surface.html, NAO index is from <https://climatedataguide.ucar.edu/climate-data/hurrell-north-atlantic-oscillation-nao-index-station-based>, AMO is from www.esrl.noaa.gov/psd/data/timeseries/AMO/and PDO is from www.ncdc.noaa.gov/teleconnections/pdo/.

All data that support the findings of this study are included within the article (and any supplementary files).

Acknowledgments

QC thanks the National Key Research and Development Program of China (Grand Nos. 2016YFC1401800, 2016YFC1401409, 2016YFC1401405, and 2017YFC1404000). JW and JO appreciate support from NOAA GOMO Arctic Research Program. This is NOAA GLERL contribution number 1961 and CIGLR contribution number 1171. Funding was awarded to the CIGLR through the NOAA Cooperative Agreement with the University of Michigan (NA17OAR4320152). We appreciate Ms Nicole Rice of NOAA GLERL for editing this article.

ORCID iD

James Overland  <https://orcid.org/0000-0002-2012-8832>

References

- Alekseev G, Glok N and Smirnov A 2016 On assessment of the relationship between changes of sea ice extent and climate in the Arctic *Int. J. Climatol.* **36** 3407–12
- Boisvert L N, Wu D L and Shie C-L 2015 Increasing evaporation amounts seen in the Arctic between 2003 and 2013 from AIRS data *J. Geophys. Res. Atmos.* **120** 6865–81
- Brennan M K, Hakim G J and Blanchard-Wrigglesworth E 2020 Arctic sea-ice variability during the instrumental era *Geophys. Res. Lett.* **47** e2019GL086843
- Chapman W C and Walsh J E 1993 Recent variations of sea ice and air temperature in high latitudes *Bull. Am. Meteorol. Soc.* **74** 33–47
- Connolly R, Connolly M and Soon W 2017 Re-calibration of Arctic sea ice extent datasets using Arctic surface air temperature records *Hydrol. Sci. J.* **62** 1317–40
- Deser C, Walsh J E and Timlin M S 2000 Arctic sea ice variability in the context of recent atmospheric circulation trends *J. Clim.* **13** 617–33
- Ding Q et al 2017 Influence of high-latitude atmospheric circulation changes on summertime Arctic sea ice *Nat. Clim. Change* **7** 289–95
- Enfield D B, Mestas-Nunez A M and Trimble P J 2001 The Atlantic multidecadal oscillation and its relationship to rainfall and river flows in the continental U.S. *Geophys. Res. Lett.* **28** 2077–80
- Gong T and Luo D 2017 Ural blocking as an amplifier of the Arctic sea ice decline in winter *J. Clim.* **30** 2639–54
- Graversen R G and Burtu M 2016 Arctic amplification enhanced by latent energy transport of atmospheric planetary waves *Quart. J. Roy. Meteor. Soc.* **142** 2046–54
- Hegyi B M and Taylor P C 2018 The unprecedented 2016–2017 Arctic sea ice growth season: the crucial role of atmospheric rivers and longwave fluxes *Geophys. Res. Lett.* **45** 52014–5212
- Hurrell J W 1995 Decadal trends in the North Atlantic Oscillation: regional temperatures and precipitation *Science* **269** 676–9
- Ikeda M, Wang J and Makshtas A 2003 Importance of clouds to the decaying trend in the Arctic ice cover *J. Meteorol. Soc. Japan.* **81** 179–89
- Kalnay E et al 1996 The NCEP/NCAR 40 year reanalysis project *Bull. Am. Meteorol. Soc.* **77** 437–70
- Kapsch M L, Graversen R G, Tjernstrom M and Bintanja R 2016 The effect of downwelling longwave and shortwave radiation on Arctic summer sea ice *J. Clim.* **29** 1143–59
- Kinnard C, Zdanowicz C M, Fisher D A, Isaksson E, Vernal A D and Thompson L G 2011 Reconstructed changes in Arctic sea ice over the past 1450 years *Nature* **479** 509–12
- Lei R, Tian-Kunze X, Lepparanta M, Wang J, Kaleschke L and Zhang Z 2016 Changes in summer sea ice, albedo, and partitioning of surface solar radiation in the Pacific sector of Arctic Ocean during 1982–2009 *J. Geophys. Res. Oceans* **121** 5470–86
- Livezey R E and Mo K C 1987 Tropical–extratropical teleconnections during the Northern Hemisphere winter. Part II: relationships between monthly mean Northern Hemisphere circulation patterns and proxies for tropical convection *Mon. Weather Rev.* **115** 3115–32
- Mác P and Pasalodos J A C 2016 Nueva serie de extensión del hielo marino ártico en septiembre entre 1935 y 2014 *Rev. Climatol.* **16** 1–19
- Mantua N J, Hare S R, Zhang Y, Wallace J M and Francis R C 1997 A Pacific interdecadal climate oscillation with impacts on salmon production *Bull. Am. Meteorol. Soc.* **78** 1069–79
- Meier W, Fetterer F and Windnagel A K 2017 Near-real-time NOAA/NSIDC climate data record of passive microwave sea ice concentration version 1 Boulder Colorado USA (<https://doi.org/10.7265/N5FF3QJ6>)
- Mewes D and Jacobi C 2019 Heat transport pathways into the Arctic and their connections to surface air temperatures *Atmos. Chem. Phys.* **19** 3927–37
- Min S-K, Zhang X Z, Wiers F W and Agnew T 2008 Human influence on Arctic sea ice detectable from early 1990s onwards *Geophys. Res. Lett.* **35** L21701
- Morice C P, Kennedy J J, Rayner N A and Jones P D 2012 Quantifying uncertainties in global and regional temperature change using an ensemble of observational estimates: the HadCRUT4 dataset *J. Geophys. Res. Atmos.* **117** 8101
- Mysak L A, Manak D K and Marsden R F 1990 Sea-ice anomalies observed in the Greenland and Labrador Seas during 1901–1984 and their relation to an interdecadal Arctic climate cycle *Clim. Dyn.* **5** 111–33
- Ogi M, Yamazaki K and Wallace J M 2010 Influence of winter and summer surface wind anomalies on summer Arctic sea ice extent *Geophys. Res. Lett.* **37** L07701
- Overland J E and Wang M 2005 The third Arctic climate pattern: 1930s and early 2000s *Geophys. Res. Lett.* **32** L23808
- Overland J E and Wang M 2015 Increased variability in the early winter subarctic North American atmospheric circulation *J. Clim.* **28** 7297–305
- Park H S, Lee S, Son S W, Feldstein S B and Kosaka Y 2015 The impact of poleward moisture and sensible heat flux on Arctic winter sea ice variability *J. Clim.* **28** 5030–9
- Peng G, Meier W, Scott D and Savoie M 2013 A long-term and reproducible passive microwave sea ice concentration data record for climate studies and monitoring *Earth Syst. Sci. Data* **5** 311–8
- Pithan F and Mauritsen T 2014 Arctic amplification dominated by temperature feedbacks in contemporary climate models *Nat. Geosci.* **7** 181–4

- Polyakov I V, Walsh J E and Kwok R 2012 Recent changes of Arctic multiyear sea ice coverage and the likely causes *Bull. Am. Meteorol. Soc.* **93** 145–51
- Rigor I G 2002 Response of sea ice to the Arctic Oscillation *J. Clim.* **15** 2648–63
- Schweiger A J, Wood K R and Zhang J 2019 Arctic sea ice volume variability over 1901–2010: a model-based reconstruction *J. Clim.* **32** 4731–52
- Screen J A and Francis J A 2016 Contribution of sea-ice loss to Arctic amplification is regulated by Pacific Ocean decadal variability *Nat. Clim. Change* **6** 856–60
- Screen J A and Simmonds I 2010 The central role of diminishing sea ice in recent Arctic temperature amplification *Nature* **464** 1334–7
- Slivinski L C et al 2019 Towards a more reliable historical reanalysis: improvements for version 3 of the twentieth century reanalysis system *Q. J. R. Meteorol. Soc.* **145** 2876–908
- Stroeve J C, Serreze M C, Holland M M, Kay J E, Malanik J and Barrett A P 2012 The Arctic's rapidly shrinking sea ice cover: a research synthesis *Clim. Change* **110** 1005–27
- Stroeve J, Holland M M, Meier W, Scambos T and Serreze M 2007 Arctic sea ice decline: faster than forecast *Geophys. Res. Lett.* **34** L09501
- Vinnikov K Y et al 1999 Global warming and Northern Hemisphere sea ice extent *Science* **286** 1934–7
- Walsh J E 1983 Role of sea ice in climate variability: theories and evidence *Atmos. Ocean* **21** 229–42
- Walsh J E, Fetterer F, Stewart J S and Chapman W L 2017 A database for depicting Arctic sea ice variations back to 1850 *Geogr. Rev.* **107** 89–107
- Wang J and Ikeda M 2000 Arctic oscillation and Arctic sea-ice oscillation *Geophys. Res. Lett.* **27** 1287–90
- Wang J and Ikeda M 2001 Arctic sea-ice oscillation: regional and seasonal perspectives *Ann. Glaciol.* **33** 481–92
- Wang J, Ikeda M, Zhang S and Gerdes R 2005 Linking the northern hemisphere sea ice reduction trend and the quasi-decadal Arctic sea ice oscillation *Clim. Dyn.* **24** 115–30
- Wang J 2014 Abrupt climate changes and emerging ice-ocean processes in the Pacific Arctic region and the Bering Sea *The Pacific Arctic Region: Ecosystem Status and Trends in a Rapidly Changing Environment* ed M J Grebmeier et al (Berlin: Springer) pp 65–100
- Wang J, Zhang J, Watanabe E, Ikeda M, Mizobata K, Walsh J E, Bai X and Wu B 2009 Is the dipole anomaly a major driver to record lows in the Arctic sea ice extent *Geophys. Res. Lett.* **36** L05706
- Wu B, Wang J and Walsh J E 2006 Dipole anomaly in the winter Arctic atmosphere and its association with Arctic sea ice motion *J. Clim.* **19** 210–25